

Crossover from Boltzmann to Wigner thermal transport in thermoelectric skutterudites

Enrico Di Lucente,¹ Michele Simoncelli,² and Nicola Marzari^{1,3}

¹*Theory and Simulation of Materials (THEOS) and National Centre for Computational Design and Discovery of Novel Materials (MARVEL), École Polytechnique Fédérale de Lausanne, Lausanne 1015, Switzerland*

²*TCM Group, Cavendish Laboratory, University of Cambridge, 19 JJ Thomson Avenue, Cambridge, CB3 0HE UK*

³*Laboratory for Materials Simulations, Paul Scherrer Institut, 5232 Villigen PSI, Switzerland*

(Dated: March 14, 2023)

Skutterudites are crystals with a cage-like structure that can be augmented with filler atoms (“rattlers”), usually leading to a reduction in thermal conductivity that can be exploited for thermoelectric applications. Here, we leverage the recently introduced Wigner formulation of thermal transport to elucidate the microscopic physics underlying heat conduction in skutterudites, showing that filler atoms can drive a crossover from the Boltzmann to the Wigner regimes of thermal transport, *i.e.*, from particle-like conduction to wave-like tunnelling. At temperatures where the thermoelectric efficiency of skutterudites is largest, wave-like tunneling can become comparable to particle-like propagation. We define a Boltzmann deviation descriptor able to differentiate the two regimes and relate the competition between the two mechanisms to the materials’ chemistry, providing a design strategy to select rattlers and identify optimal compositions for thermoelectric applications.

Heat is a waste product of many and diverse energy intensive technologies, from vehicle exhausts in transportation to nuclear and natural gas power plants production, to large-scale manufacturing. Ongoing research is focused on finding strategies to convert such waste heat into electricity, and thermoelectric materials are among the most promising candidates [1] for this task, and for augmenting sustainable energy supplies in the near future. The thermoelectric figure of merit reaches a record value of 3.1 at 783 K in polycrystalline SnSe [2], even greater than the value obtained for single crystals [3] due to enhanced scattering. While many efforts have focused on designing materials with enhanced thermoelectric performance [4, 5], understanding how to maximise energy-conversion efficiency by decreasing thermal conductivity has been hindered by the lack of a microscopic theory capturing the mechanisms of heat conduction in poor thermal conductors. Fittingly, the recently developed Wigner formulation of thermal transport [6, 7] allows to describe heat conduction in anharmonic crystals and in solids with ultralow or glass-like conductivity; this is exactly the case of thermoelectrics. The Wigner formulation offers a comprehensive approach to describe heat transport across different regimes, covering on the same footing harmonic “Boltzmann crystals”, anharmonic “Wigner crystals” and amorphous solids and glasses. A Boltzmann crystal is characterized by phonon interband spacings much

larger than the phonon linewidths; in Boltzmann crystals particle-like heat conduction dominates [6–8] and the Peierls-Boltzmann transport equation [9, 10] describes accurately thermal conductivity [11, 12]. In amorphous solids and glasses wave-like tunneling dominates and the Wigner formulation recovers the Allen-Feldman formulation [13] accounting also for anharmonicity [14]. Last, Wigner crystals can be considered as the intermediate regime between the first two and are characterized by interband spacings which are comparable to phonon linewidths. The Peierls-Boltzmann equation fails to describe the wave-like contributions [15–18] in materials with ultralow thermal conductivity, that are captured by the Wigner transport equation [6, 7].

Among others, skutterudites have been extensively studied for their possible applications in thermoelectrics [19–21] showing both high electrical and low thermal conductivities. The cage-like structure of skutterudites is a critical feature for thermoelectricity [21, 22]: the voids present in the structure can be occupied by loosely bound atoms (“fillers” or “rattlers”) that can reduce thermal conductivity and enhance the thermoelectric figure of merit [23]. However, the interpretation of filler vibrations remain controversial [16, 37, 38]; here, we aim to clarify the fundamental mechanisms behind the reduction of thermal conductivity – and thus the related thermoelectric performance – applying the Wigner transport equation and its resulting lattice thermal conductivity

$\kappa_{\text{tot}}^{\alpha\beta}$:

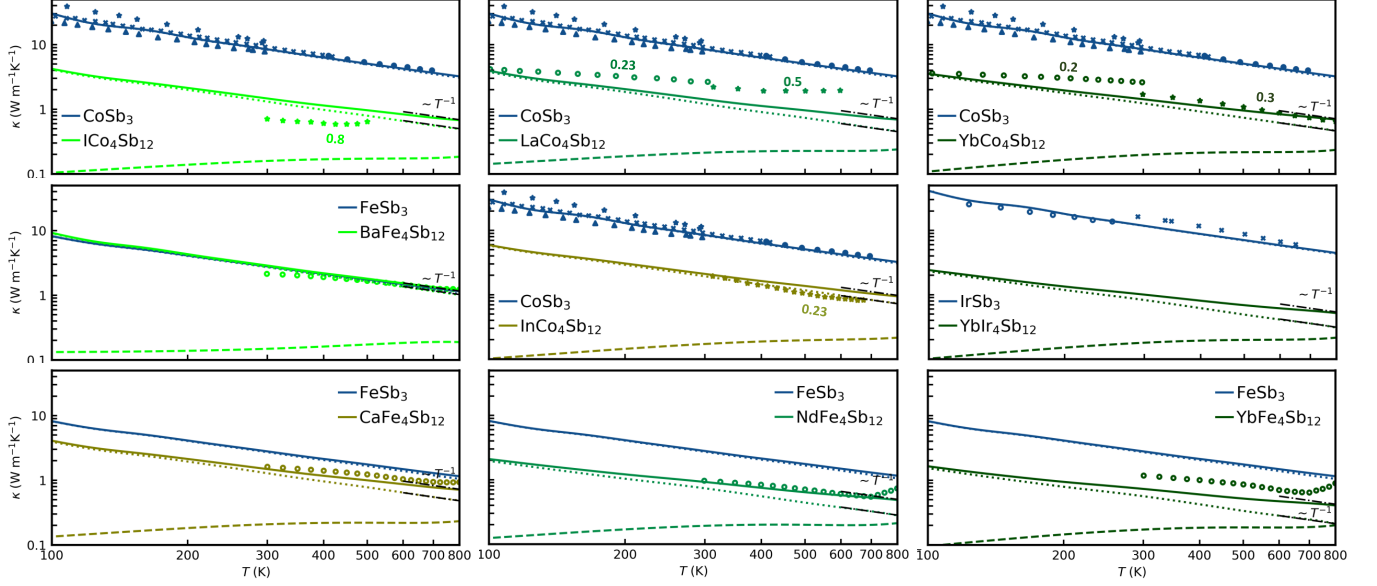


Figure 1: Calculated κ_{tot} (solid), κ_P (dotted) and κ_C (dashed) for unfilled FeSb_3 , CoSb_3 and IrSb_3 and for their related filled compounds $\text{RFe}_4\text{Sb}_{12}$ ($\text{R} = \text{Ba}, \text{Ca}, \text{Nd}, \text{Yb}$), $\text{RCo}_4\text{Sb}_{12}$ ($\text{R} = \text{I}, \text{In}, \text{La}, \text{Yb}$) and $\text{RIr}_4\text{Sb}_{12}$ ($\text{R} = \text{Yb}$), between 100 and 800 K. Experimental κ_{tot} are taken from Refs. [24] for $\text{RFe}_4\text{Sb}_{12}$ ($\text{R} = \text{Ba}, \text{Ca}, \text{Nd}, \text{Yb}$), [25, 26] for CoSb_3 , [27, 28] for $\text{ICo}_4\text{Sb}_{12}$, [29] for $\text{InCo}_4\text{Sb}_{12}$, [30, 31] for $\text{LaCo}_4\text{Sb}_{12}$, [32, 33] for $\text{YbCo}_4\text{Sb}_{12}$ and [34, 35] for IrSb_3 . Symbols represent different experimental measurements, also color-coded according to the material. Experimental data referring to partial concentration of the filler are specified adjacent to the symbols. The universal T^{-1} trend of κ_P [16, 36] is also shown; κ_{tot} displays a milder decay than κ_P .

$$\kappa_{\text{tot}}^{\alpha\beta} = \kappa_{\text{P,SMA}}^{\alpha\beta} + \frac{1}{(2\pi)^3} \int_{\text{BZ}} \sum_{s \neq s'} \frac{\omega(\mathbf{q})_s + \omega(\mathbf{q})_{s'}}{4} \left[\frac{C(\mathbf{q})_s}{\omega(\mathbf{q})_s} + \frac{C(\mathbf{q})_{s'}}{\omega(\mathbf{q})_{s'}} \right] v^\alpha(\mathbf{q})_{s,s'} v^\beta(\mathbf{q})_{s',s} \frac{\frac{1}{2} [\Gamma(\mathbf{q})_s + \Gamma(\mathbf{q})_{s'}]}{[\omega(\mathbf{q})_{s'} - \omega(\mathbf{q})_s]^2 + \frac{1}{4} [\Gamma(\mathbf{q})_s + \Gamma(\mathbf{q})_{s'}]^2} d^3q, \quad (1)$$

where $\omega(\mathbf{q})_s$ is the angular frequency of a phonon having wavevector \mathbf{q} and mode s , $C(\mathbf{q})_s = \frac{\hbar^2 \omega^2(\mathbf{q})_s}{k_B T^2} \bar{N}(\mathbf{q})_s [\bar{N}(\mathbf{q})_s + 1]$ is the specific heat of that phonon population, $\bar{N}(\mathbf{q})_s$ is the equilibrium Bose-Einstein distribution at temperature T , $v^\alpha(\mathbf{q})_{s,s'}$ and $v^\beta(\mathbf{q})_{s',s}$ are the cartesian components of the velocity operator, which generalizes the concept of group velocity, and $\Gamma(\mathbf{q})_s = \frac{1}{\tau(\mathbf{q})_s}$ is the phonon linewidth of a phonon with lifetime $\tau(\mathbf{q})_s$. The symbol BZ in Eq. (1) represents an integral over the Brillouin zone. $\kappa_{\text{P,SMA}}^{\alpha\beta}$ in Eq. (1) is the Peierls-Boltzmann particle-like conductivity, which is driven by phonon-phonon scattering in the single-mode relaxation time approximation (SMA). The additional Wigner term in Eq. (1) is a positive-definite tensor ($\kappa_C^{\alpha\beta}$) emerging from the phase “coherences” between pairs of phonon eigenstates; *i.e.*, from the wave-tunneling between two nondegenerate bands ($s \neq s'$) [39, 40]. In order to explore the relative strength of the particle-like and wave-like heat-conduction mechanisms, we study three different families of skutterudites, where we compute from first-principles (see Supplementary Information (SI) [41] for details) all the quantities needed to evaluate Eq. (1) for unfilled FeSb_3 , CoSb_3 and IrSb_3 , and for

the filled compounds $\text{RFe}_4\text{Sb}_{12}$ ($\text{R} = \text{Ba}, \text{Ca}, \text{Nd}, \text{Yb}$), $\text{RCo}_4\text{Sb}_{12}$ ($\text{R} = \text{I}, \text{In}, \text{La}, \text{Yb}$) and $\text{RIr}_4\text{Sb}_{12}$ ($\text{R} = \text{Yb}$). We note, in passing, that skutterudites contain elements for which DFT+U [43–46] might improve upon self-interaction errors for localized electrons [47]; these aspects are discussed in the SI [41].

The resulting thermal conductivities, together with their good agreement with the available experimental data, are shown in Fig. 1 in the temperature range from 100 to 800 K. By focusing on the high-performance high-temperature regime ($T \geq 600\text{K}$) and comparing κ_P and κ_C , it is clearly seen how unfilled skutterudites behave as Boltzmann crystals, displaying dominant particle-like conduction. Moreover, in the high-temperature region, $\kappa \simeq \kappa_P \propto T^{-1}$, as predicted by the Peierls-Boltzmann equation [36, 48]. On the other hand, for filled skutterudites, the behaviour is that of a Wigner crystal, with a milder decay of κ_{tot} as also observed for many highly anharmonic crystals [16, 17, 49]. We highlight how Yb-filled materials show a stronger Wigner-crystal behavior, *i.e.* $\kappa_P \sim \kappa_C$, while for $\text{BaFe}_4\text{Sb}_{12}$ the behaviour is more similar to that of a Boltzmann crystal, *i.e.* $\kappa_P > \kappa_C$. It is worth noting that some experimental measurements show an increase in conductivity at very high temperatures ($\geq 700\text{K}$); this could be

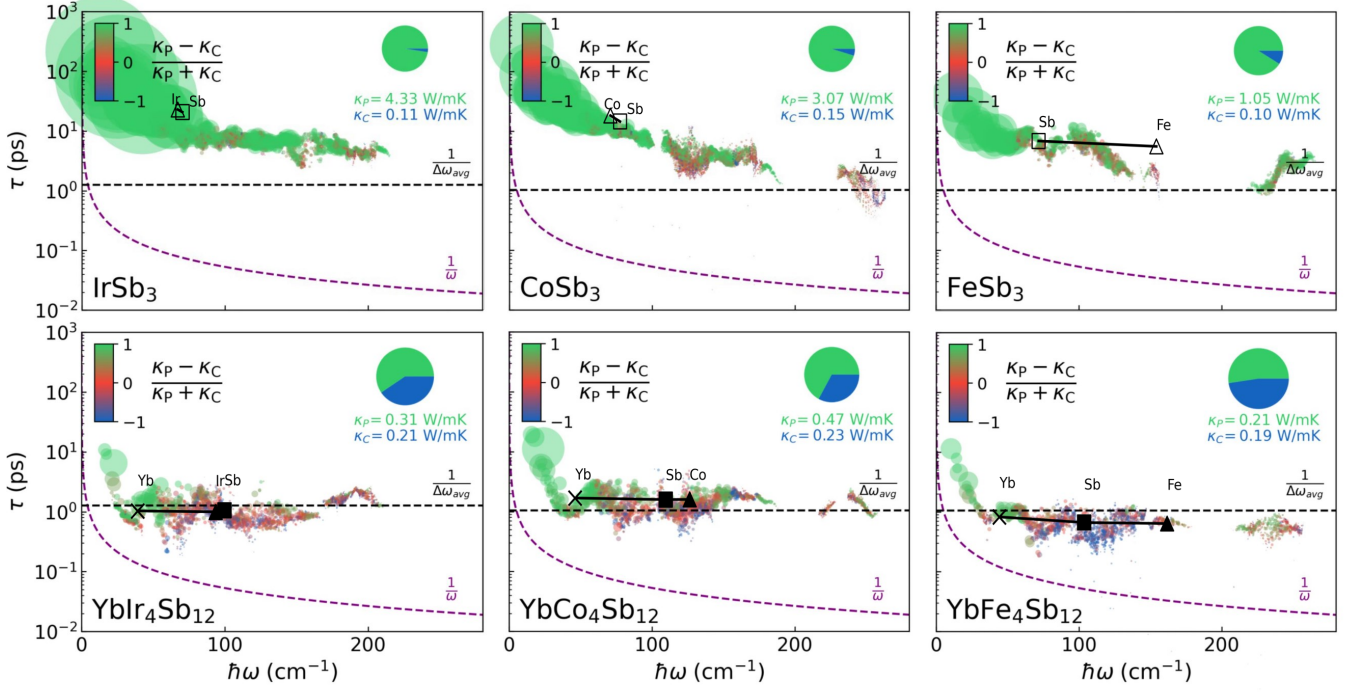


Figure 2: Distribution of phonon lifetimes $\tau(\mathbf{q})_s = \Gamma(\mathbf{q})_s^{-1}$ as a function of energy $\hbar\omega(\mathbf{q})_s$ for unfilled (upper panels) and Yb-filled (lower panels) skutterudites at 800 K. The area of each scatter point is proportional to the contribution to the total lattice thermal conductivity and colored according to the origin of the contribution: $c = [\kappa_P^{\text{avg}}(\mathbf{q})_s - \kappa_C^{\text{avg}}(\mathbf{q})_s] / [\kappa_P^{\text{avg}}(\mathbf{q})_s + \kappa_C^{\text{avg}}(\mathbf{q})_s]$, where particle-like is green ($c = 1$), wave-like is blue ($c = -1$) and intermediate mechanisms have intermediate colors, with red corresponding to 50% of particle-like and 50% of wave-like contributions [7]. The Wigner limit in time (dashed-black line) corresponds to a phonon lifetime equal to the inverse of the average interband spacing ($\tau^\omega = \Delta\omega_{\text{avg}}^{-1}$). The dashed-purple hyperbola shows the Ioffe-Regel limit in time [7, 42] ($\tau^{\text{IR}} = \omega^{-1}$), below which phonons are no longer well-defined quasi-particles. The pie charts have an area proportional to the total lattice thermal conductivity, and the slices resolve the particle-like conductivity (green) and the wave-like conductivity (blue). The black symbols connected by black lines are the points whose coordinates are the average energies and lifetimes projected on atoms (see SI [41]). Open (closed) symbols refer to unfilled (filled) skutterudites. The projections on the filler, transition-metal and antimony atoms are given by crosses, triangles and squares, respectively. The phonon lifetimes distribution for the remaining filled skutterudites are given in the SI [41].

understood as driven by radiative and electronic heat transfer [50, 51], unrelated to the increase in coherences' conductivity. At high temperatures, radiative effects on thermal transports are expected to be important because radiative thermal conductivity should increase as T^3 [52], while in semiconductors the electronic contribution can be important when, as temperature rises, electrons are excited to the conduction band [51].

In order to elucidate the physics underlying the low thermal conductivity of efficient thermoelectric skutterudites, we make a comparison between phonon lifetimes and average phonon interband spacing $\Delta\omega_{\text{avg}} = \frac{\omega_{\text{max}}}{3N_{\text{at}}}$ (ω_{max} being the maximum phonon frequency and N_{at} the number of atoms in the primitive cell) [7], to describe how much each phonon contributes to the wave-like vs. the particle-like conduction mechanisms. As shown in Ref. [7], the ratio between the two is approximately equivalent to the ratio between the phonon linewidth

and the average phonon interband spacing,

$$\frac{\kappa_C^{\text{avg}}(\mathbf{q})_s}{\kappa_P^{\text{avg}}(\mathbf{q})_s} \simeq \frac{\Gamma(\mathbf{q})_s}{\Delta\omega_{\text{avg}}} = \frac{1}{\tau(\mathbf{q})_s \Delta\omega_{\text{avg}}}. \quad (2)$$

From this one can define the Wigner limit in time $\tau^\omega = \frac{1}{\Delta\omega_{\text{avg}}}$, that determines the crossover from a regime of dominant particle-like conduction to one of dominant wave-like conduction.

In Fig. 2 we show the distribution $\tau(\mathbf{q})_s$ of the phonon lifetimes as a function of the energy $\hbar\omega(\mathbf{q})_s$ for the unfilled (upper panels) and Yb-filled (lower panels) skutterudites at 800 K. Phonons above the Wigner limit in time (*i.e.* with $\tau(\mathbf{q})_s > \tau^\omega$) contribute mainly to particle-like conductivity, while phonons below this limit (*i.e.* with $\tau(\mathbf{q})_s < \tau^\omega$) contribute mainly to the wave-like conductivity. We note that in all the compounds studied [41] the phonon lifetimes sit well above the Ioffe-Regel limit in time $\tau^{\text{IR}} = \omega^{-1}$ [7] (dashed-purple), confirming that phonons in these materials are well defined quasi particles and that the Wigner formulation is valid

[7]. If this were not the case, then full spectral function approaches [53, 54] would be required. The clouds of phonon lifetimes in Fig. 2 remain distinctly above the Wigner limit for the unfilled compounds, while they are centered around the Wigner limit for the Yb-filled compounds. This allows to identify the crossover from the Boltzmann-crystal behaviour of unfilled skutterudites to the Wigner-crystal behaviour of Yb-filled ones, where phonon coherences become significant. Moreover, Fig. 2 also shows the atom-resolved energies and lifetimes (see Eqs. 3 and 4 of SI [41]), indicating how, in general, different atoms contribute to different regions of the distribution. We see that Yb fillers drive the characteristic lifetimes towards the Wigner limit in time, while the characteristic energies of the Ir/Co/Fe atoms, and of Sb are only slightly shifted higher. Given a certain phonon lifetime, the frequency associated to the filler is significantly lower than that of the other atom types in the structure, suggesting that indeed Yb behaves like a rattler [55]. These findings extend those discussed in Ref. [16], where it was suggested that fillers interact with the host matrix coherently, albeit without resolving the single-atom contributions in the energy-lifetime distribution. In fact, the present analysis shows how filling with Yb lowers all the lifetimes, not only those of the filler itself.

Then, we want to describe how each chemical species that composes the skutterudite structure influences the relative strengths of κ_P and κ_C . Since the Boltzmann or Wigner crystal behaviour is regulated by the competition between the phonon lifetimes and the Wigner limit in time [7] (see Eq. (2)), we introduce a Boltzmann deviation descriptor (B) defined as the inverse of the product between the skutterudite characteristic lifetime – *i.e.* the Matthiessen's sum of the average lifetimes resolved on atom types (see SI [41] for details) – and the average phonon interband spacing [7]:

$$B = \frac{1}{\bar{\tau}\Delta\omega_{\text{avg}}} = \begin{cases} \frac{1}{\tau^U\Delta\omega_{\text{avg}}}, & \text{with } \tau^U = \frac{\tau_M\tau_{\text{Sb}}}{\tau_M + \tau_{\text{Sb}}} \\ \frac{1}{\tau^F\Delta\omega_{\text{avg}}}, & \text{with } \tau^F = \frac{\tau_R\tau_M\tau_{\text{Sb}}}{\tau_R\tau_M + \tau_R\tau_{\text{Sb}} + \tau_M\tau_{\text{Sb}}}, \end{cases} \quad (3)$$

where $\bar{\tau}$ is the average lifetime [41], F and U superscripts symbolize filled and unfilled skutterudites, R the rattler, and M the Ir/Co/Fe metal.

In the upper panel of Fig. 3 we show the correlation between $\frac{\kappa_P}{\kappa_C}$ and B at 800 K. Interestingly, we find to a good approximation the power relation: $\frac{\kappa_P}{\kappa_C} \simeq B^{-\frac{3}{4}}$. It can be shown analytically [41] that for a constant DOS, $\frac{\kappa_P}{\kappa_C} = B^{-1}$; so, we can attribute the $-3/4$ exponent (< 1) to the fact that the real DOS is not constant. Finally, we want to understand how skutterudites' chemistry comes into play in discriminating the ability of the filler atom to move inside the cage and how this is related to B . The mean-square displacement (MSD) is often used in the literature to describe vibrating systems characterized by loosely bound atoms with long and elongated bonds

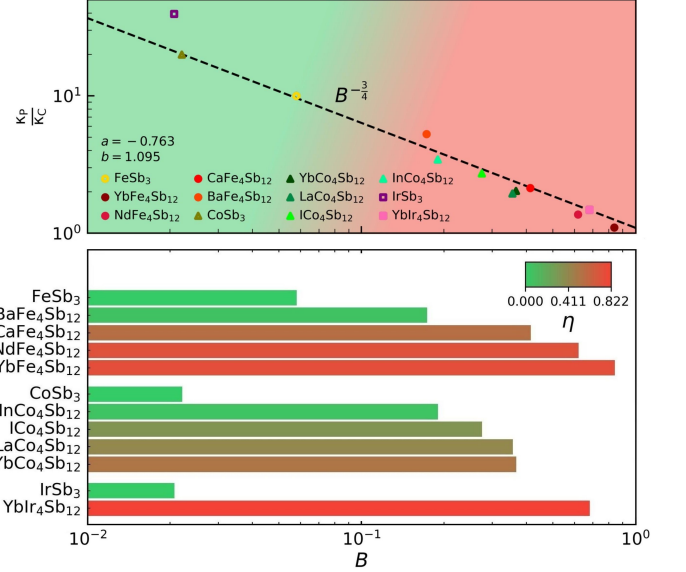


Figure 3: (Upper panel) Relation between the relative strength of particle-like and wave-like conduction ($\frac{\kappa_P}{\kappa_C}$) at 800 K and B as given in Eq. (3); unfilled (filled) symbols represent unfilled (filled) skutterudites. Circles, triangles and squares represent Fe-, Co- and Ir-based skutterudites respectively. The black dashed line corresponds to the $\frac{\kappa_P}{\kappa_C} = B^{-\frac{3}{4}}$ power law interpolating the data. The shaded regions show a smooth crossover from a dominant particle-like heat conduction in green, to a competing particle- and wave-like mechanism in red. (Lower panel) Histogram of the B values obtained for all the skutterudites studied. The color scale is given by the descriptor η of Eq. (4). The correlation between B and η shows how skutterudites' chemistry determines the degree of Wigner thermal transport in these materials.

[41, 56]. From this follows that the ratio between the MSD of the filler atom (MSD_R) and that of the cage atoms (MSD_{Sb}) can be used to quantify the relative effect of the filler atom's vibrations in the host structure. On the other hand, the ratio between the filler-cage atoms distance and the average bond length of the structure keeps track of the nature of the chemical bond, *i.e.*, the effective distance along which the filler can move. We can then define a heuristic parameter that describes how the relative structural oscillations of the filler atom vary depending on the length of the chemical bonds it affects:

$$\eta = \frac{\text{MSD}_R}{\text{MSD}_{\text{Sb}}} \frac{d_{\text{Sb-R}}}{d_{\text{avg}}}, \quad (4)$$

where $d_{\text{Sb-R}}$ is the distance between the filler atom and the atoms of the cage and d_{avg} is the average bond length of the structure.

In the lower panel of Fig. 3 we show the distribution of B obtained for each of the materials studied. This confirms the trend obtained for $\frac{\kappa_P}{\kappa_C}$ in the upper panel of Fig. 3, and validates numerically the predictions from Eq. (2). Most importantly, η (used for the color scale) allows to connect the physics behind Wigner heat trans-

port to the chemistry of the skutterudites: the larger the B , the larger η . This underscores how B is proportional to the rattling motion of the filler, quantified by MSD_R , and is therefore able to distinguish between optimal filler atoms for the reduction of κ_{tot} from those for which the thermal behavior remains similar to that of unfilled skutterudites. *E.g.*, the filled skutterudite $\text{BaFe}_4\text{Sb}_{12}$ behaves very close to a Boltzmann crystal, since its η is significantly lower than that of the other filled skutterudites. We also observe that a rescaling of the filler's atomic weight translates into negligible changes of κ_{tot} , thus confirming that thermal transport is determined by bonding chemistry [41]. In the end, it is worth noting that only the MSDs (harmonic properties) and the crystal chemical bonds enter the definition of η , and thus already at this level it might be possible to predict the degree of Wigner behavior of a thermoelectric material. Since harmonic properties are much less computationally demanding than anharmonic ones, one could screen for thermoelectric materials with a strong wave-like contribution to conductivity through the descriptor η , at least for cage-like materials showing rattling motion.

In conclusion, we have used the Wigner formulation of thermal transport to investigate the microscopic physics underlying heat conduction in skutterudites, showing a crossover from Boltzmann to Wigner thermal transport when filling with, *e.g.*, Yb atoms. Unfilled skutterudites behave as Boltzmann crystals, while filled ones change behavior from Boltzmann to Wigner depending on the filler atom and its bonding properties. We showed that, given the same host structure, the materials displaying the lowest conductivity are precisely those in which the $\frac{\kappa_P}{\kappa_C}$ ratio between particle-like and wave-like contributions is larger. We also elucidated how the degree of Wigner heat conduction is correlated to the relative motion between the filler atom and the cage; the latter being dependent on the chemical composition of the skutterudite structure. This study paves the way for the identification of the most suitable chemical compositions to engineer new and efficient cage-like thermoelectric materials.

This research was supported by the Swiss National Science Foundation (SNSF), through Grant No. CR-SII5.189924 (“Hydronics” project).

[1] G. J. Snyder and E. S. Toberer, *Nature materials* **7**, 105 (2008).
 [2] C. Zhou, Y. K. Lee, Y. Yu, S. Byun, Z.-Z. Luo, H. Lee, B. Ge, Y.-L. Lee, X. Chen, J. Y. Lee, *et al.*, *Nature materials* **20**, 1378 (2021).
 [3] L.-D. Zhao, S.-H. Lo, Y. Zhang, H. Sun, G. Tan, C. Uher, C. Wolverton, V. P. Dravid, and M. G. Kanatzidis, *nature* **508**, 373 (2014).
 [4] D. M. Rowe, *CRC handbook of thermoelectrics* (CRC press, 2018).

[5] G. A. Slack and M. A. Hussain, *Journal of applied physics* **70**, 2694 (1991).
 [6] M. Simoncelli, N. Marzari, and F. Mauri, *Nature Physics* **15**, 809 (2019).
 [7] M. Simoncelli, N. Marzari, and F. Mauri, *Physical Review X* **12**, 041011 (2022).
 [8] M. Simoncelli, N. Marzari, and A. Cepellotti, *Physical Review X* **10**, 011019 (2020).
 [9] R. Peierls, *Annalen der Physik* **395**, 1055 (1929).
 [10] R. Peierls and R. E. Peierls, *Quantum theory of solids* (Oxford University Press, 1955).
 [11] J. Garg, N. Bonini, B. Kozinsky, and N. Marzari, *Physical review letters* **106**, 045901 (2011).
 [12] D. A. Broido, M. Malorny, G. Birner, N. Mingo, and D. Stewart, *Applied Physics Letters* **91**, 231922 (2007).
 [13] P. B. Allen and J. L. Feldman, *Physical Review B* **48**, 12581 (1993).
 [14] M. Simoncelli, F. Mauri, and N. Marzari, *arXiv preprint arXiv:2209.11201* (2022).
 [15] D. Donadio and G. Galli, *Physical review letters* **102**, 195901 (2009).
 [16] W. Li and N. Mingo, *Physical Review B* **91**, 144304 (2015).
 [17] A. Weathers, J. Carrete, J. P. DeGrave, J. M. Higgins, A. L. Moore, J. Kim, N. Mingo, S. Jin, and L. Shi, *Physical Review B* **96**, 214202 (2017).
 [18] T. Zhu and E. Ertekin, *Energy & Environmental Science* **12**, 216 (2019).
 [19] E. Bauer, C. Paul, M. Della Mea, G. Hilscher, H. Michor, M. Reissner, W. Steiner, A. Grytsiv, P. Rogl, E. Scheidt, *et al.*, *Physical Review B* **66**, 214421 (2002).
 [20] P.-a. Zong, R. Hanus, M. Dylla, Y. Tang, J. Liao, Q. Zhang, G. J. Snyder, and L. Chen, *Energy & Environmental Science* **10**, 183 (2017).
 [21] M. G. Kanatzidis, T. Hogan, and S. Mahanti, *Chemistry, physics, and materials science of thermoelectric materials: beyond bismuth telluride* (Springer Science & Business Media, 2012).
 [22] C. Uher, *Materials aspect of thermoelectricity* (CRC press, 2016).
 [23] T. Tritt, *Recent trends in thermoelectric materials research, part two* (Academic Press, 2000).
 [24] P. Qiu, J. Yang, R. Liu, X. Shi, X. Huang, G. Snyder, W. Zhang, and L. Chen, *Journal of Applied Physics* **109**, 063713 (2011).
 [25] K. L. Stokes, A. Ehrlich, and G. Nolas, *MRS Online Proceedings Library Archive* **545** (1998).
 [26] Y. Kawaharada, K. Kurosaki, M. Uno, and S. Yamanaka, *Journal of alloys and compounds* **315**, 193 (2001).
 [27] X. Li, B. Xu, L. Zhang, F. Duan, X. Yan, J. Yang, and Y. Tian, *Journal of alloys and compounds* **615**, 177 (2014).
 [28] L. Zhang, B. Xu, X. Li, F. Duan, X. Yan, and Y. Tian, *Materials Letters* **139**, 249 (2015).
 [29] R. C. Mallik, C. Stiewe, G. Karpinski, R. Hassdorf, and E. Müller, *Journal of electronic materials* **38**, 1337 (2009).
 [30] G. S. Nolas, J. Cohn, and G. Slack, *Physical Review B* **58**, 164 (1998).
 [31] A. B. Mohamed Bashir, *Thermoelectric properties of $\text{LaCo}_4\text{Sb}_{12}$ skutterudite materials by addition of Al, In, Ni & Te/Mohamed Bashir Ali Bashir*, Ph.D. thesis, University of Malaya (2017).
 [32] G. Nolas, M. Kaeser, R. Littleton IV, and T. Tritt, *Ap-*

- plied Physics Letters **77**, 1855 (2000).
- [33] S. Wang, J. R. Salvador, J. Yang, P. Wei, B. Duan, and J. Yang, NPG Asia Materials **8**, e285 (2016).
 - [34] G. Nolas, G. Slack, D. Morelli, T. Tritt, and A. Ehrlich, Journal of Applied Physics **79**, 4002 (1996).
 - [35] G. A. Slack and V. G. Tsoukala, Journal of Applied Physics **76**, 1665 (1994).
 - [36] T. Sun and P. B. Allen, Physical Review B **82**, 224305 (2010).
 - [37] V. Keppens, D. Mandrus, B. C. Sales, B. Chakoumakos, P. Dai, R. Coldea, M. Maple, D. Gajewski, E. Freeman, and S. Bennington, Nature **395**, 876 (1998).
 - [38] J. Feldman, D. Singh, I. Mazin, D. Mandrus, and B. Sales, Physical Review B **61**, R9209 (2000).
 - [39] F. Rossi, *Theory of semiconductor quantum devices: microscopic modeling and simulation strategies* (Springer Science & Business Media, 2011).
 - [40] R. C. Iotti, E. Ciancio, and F. Rossi, Physical Review B **72**, 125347 (2005).
 - [41] See Supplementary Information at (link).
 - [42] A. Ioffe and A. Regel, Prog. Semicond **4**, 237 (1960).
 - [43] V. I. Anisimov, J. Zaanen, and O. K. Andersen, Physical Review B **44**, 943 (1991).
 - [44] V. I. Anisimov, F. Aryasetiawan, and A. Lichtenstein, Journal of Physics: Condensed Matter **9**, 767 (1997).
 - [45] S. Dudarev, G. Botton, S. Savrasov, C. Humphreys, and A. Sutton, Physical Review B **57**, 1505 (1998).
 - [46] E. Di Lucente and N. Marzari, Manuscript in Preparation (2023).
 - [47] H. J. Kulik, M. Cococcioni, D. A. Scherlis, and N. Marzari, Physical Review Letters **97**, 103001 (2006).
 - [48] S. Shenogin, A. Bodapati, P. Keblinski, and A. J. McGaughey, Journal of Applied Physics **105**, 034906 (2009).
 - [49] D. G. Cahill, S. K. Watson, and R. O. Pohl, Physical Review B **46**, 6131 (1992).
 - [50] J. R. Howell, M. P. Mengüç, K. Daun, and R. Siegel, *Thermal radiation heat transfer* (CRC press, 2020).
 - [51] J. M. Ziman, *Principles of the Theory of Solids* (Cambridge university press, 1972).
 - [52] H. Keppler, L. S. Dubrovinsky, O. Narygina, and I. Kantor, Science **322**, 1529 (2008).
 - [53] Đ. Dangić, O. Hellman, S. Fahy, and I. Savić, npj Computational Materials **7**, 1 (2021).
 - [54] G. Caldarelli, M. Simoncelli, N. Marzari, F. Mauri, and L. Benfatto, arXiv preprint arXiv:2202.02246 (2022).
 - [55] Z. Feng, Y. Fu, Y. Zhang, and D. J. Singh, Physical Review B **101**, 064301 (2020).
 - [56] B. Sales, B. Chakoumakos, and D. Mandrus, Physical Review B **61**, 2475 (2000).